

THE NUMERICAL SIMULATION OF
ASTROPHYSICAL JETS: THE INTERACTION
WITH SURROUNDING MEDIUMO.DONMEZ¹, A.AKTAS², U.ILTER²

Received 19 September 2016

Accepted 7 June 2017

Propagation of astrophysical jets inside the ambient medium transports the large amount of energy to surrounding materials as a consequence of interactions. These interactions have a crucial effect on the evolution and dynamic of the jets. They can cause the formation of jet's head which dissipates its energy. In this paper, we have numerically modeled the evolution of jet's dynamics to understand the effects of the critical parameters (Mach numbers, jet velocity, densities, pressures of the accelerated jet and medium, sound speeds, and Lorentz factor) on the head of jet, jet-cocoon, vortexes and shocks. When the jet propagates inside the overdense region, we observe the clear evidence for deceleration of the jet and find more complex structure. In the underdense cases, almost no back-flows and cocoons are developed. We have also modeled the pulsed type jets propagating into overdense region and found very rich internal structure of jet such as cocoon, knots, vortexes, etc. They could explain the structure of jets seen in Herbig-Haro bows and XZ Tauri proto-jet.

Key words: *numerical relativity: astrophysical jets: ambient medium: jets structure*

1. *Introduction.* The collimation of relativistic jets can be seen in different astrophysical phenomena such as active galactic nuclei (AGN), X-ray binaries, microquasars and gamma-ray bursts. They are relativistic, collimated and launched due to consequence of the rotational energy of the black hole [1]. The emission from jet was observed from the different kinds of sources [2] and their connections with the other energy bands were examined by [3]. The observations showed that the highly collimated jets with high Mach number outflows were found at protostellar and Herbig-Haro objects. The radiative shock fronts are generated during the jet flow as a consequence of the interaction with the surrounding medium.

The numerical solution of relativistic hydrodynamical equations helps in understanding the physical properties and dynamical behavior of astrophysical jets. Throughout the last few decades significant progress has been made in numerical simulations of jets. Various authors have done extensive studies on jet's collimation [4-9] and interaction of the jet with the surrounding medium [10-18]. The numerical calculations has been performed to obtain the physical properties of the

jets and the results explored that the sudden density and pressure jumps during the interaction of the jets with surrounding medium caused an instability and the rich dynamics. This instability is called Kelvin-Helmholtz instability which is derived by the shear between propagating jet and medium.

The jets in young XZ Tau binary shows the compact knots and has complex outflows. These jets have different variety of structures such as bow shocks, shells, fans etc. [19]. They assumed the large velocity pulse injections to explain the observed forms in XZ Tau A and have presented the preliminary results of the pulsed jet. The pulsed jet with high Mach number was presented in terms of interacting bow shocks, Mach disk and some instabilities observed in the jets [20].

In this paper, we have done a sequence of numerical simulations of astrophysical jets, motivated by common predictions from the general scenario of outflowing jets inside the surrounding medium. We present the results of 2D numerical simulations of relativistic jets to uncover the dynamics and their interactions with the surrounding medium by focusing on certain scenarios observed in jets. We present the results of series of long-term projects devoted to understand the dynamics and emission of jets in parsec-scale AGN jets, blazars, young XZ Tau binary and the afterglow phase of the GRBs. Galactic and extragalactic relativistic jets are surrounded by rich environments that are full of moving objects, such as stars and dense medium inhomogeneities.

This paper is organized as follows: the general overview of hydrodynamic equation, the initial setup of astrophysical jets, and the numerical setup and boundary conditions are provided in Section 2. In section 3, we describe our numerical results about jet's dynamics and their time consuming behavior. Detail discussions are made to understand the parameter dependences of astrophysical jets and their interaction with surrounding medium. Finally, we conclude our findings in Section 4. The geometrized unit system, $c=1$ and $G=1$, is used to have a simpler relativistic equations.

2. Equations, numerical setups, boundaries and initial conditions.

2.1. *Equations.* The special relativistic hydrodynamical equation is solved by using the high resolution shock capturing scheme to model astrophysical jet problems around the compact objects. The equation can be written in 2D as

$$\frac{\partial \mathbf{U}}{\partial t} + \frac{\partial \mathbf{F}^z}{\partial z} + \frac{\partial \mathbf{F}^R}{\partial y} = 0, \quad (1)$$

where \mathbf{U} , \mathbf{F}^z and \mathbf{F}^R represent the conserved variable and fluxes along the jet axis and axis perpendicular to jet axis, respectively. The full set of general relativistic hydrodynamical equations and detail explanation about their numerical solutions are discussed in detail [13] and [21].

2.2. *Initial data for astrophysical jets.* We have performed 2D numerical simulation of the jets to understand the dynamical change of them using different values of parameters of matters injected close to the compact object and parameters for surrounding, given in Tables 1 and 2, respectively. The injected matter moves along the axis z is called the jet axis. R is direction perpendicular to jet axis, z . The matter is injected along the jet axis in a distance $3M$ from the compact object, where M is the mass of the black hole. The compact object stays at the same position during the simulation time which varies for every model given in Table 1. We have neglected the influence of magnetic field on the jet dynamics and matter is injected continuously during the simulation.

Columns in Table 1 present the model name, C_s - speed of sound, Γ - the adiabatic index of the injected matter, V_z - the speed of injected matter, M - the Mach number of the matter, ρ - the rest-mass density, p - the pressure which is computed from Eq. (2), CFL is CFL number and AM represents the ambient medium which is given in Table 2.

Table 1

INITIAL VALUES OF INJECTED MATTER AT $z = 2.8 M$ ALONG THE z DIRECTION

Model	C_s	Γ	V_z	M	ρ	p	CFL	AM
JOr1R0	0.01	4/3	0.9	90	10^5	7.50225×10^{10}	0.05	Or1
JOr1R1	0.05	4/3	0.9	90	10^5	1.88916×10^8	0.05	Or1
JOr1R2	0.1	4/3	0.9	90	10^5	7.73196×10^4	0.04	Or1
JOr2R3	0.01	5/3	0.9	90	10^5	6.00089×10^{10}	0.03	Or2
JOr2R4	0.1	5/3	0.9	90	10^5	6.09137×10^8	0.03	Or2
JOr3R5	0.01	1.2	0.9	90	10^5	8.33350×10^{10}	0.05	Or3
JOr3R6	0.01	1.2	0.99	99	10^5	8.33350×10^{10}	0.01	Or3
JOr4R7	0.01	4/3	0.9	90	10^3	7.50225×10^8	0.01	Or4
JOr5R8	0.01	5/3	0.9	90	10^3	6.00090×10^8	0.005	Or5
JOr6R9	0.01	2	0.9	90	10^3	5.00049×10^8	0.005	Or6
JOr7R10	0.01	4/3	0.9	90	10^3	5.05050×10^8	0.05	Or7
JOr7R11	0.001	4/3	0.9	90	10^3	5.00000×10^{10}	0.05	Or7
JOr7R12*	0.01	4/3	0.1	10	10^3	5.00500×10^8	0.05	Or7
JOr7R13*	0.01	4/3	0.1	10	10^3	5.00500×10^8	0.05	Or7
JOr7R14*	0.01	4/3	0.9	90	10^3	5.00500×10^8	0.05	Or7

* They have the same initial conditions but the pulsation time of injected matter are different.

Columns in Table 2 present AM - the name of ambient medium, C_s - the speed of sound, Γ - the adiabatic index of the ambient medium, V - the speed of the matter at ambient medium, ρ - the rest-mass density and p - the pressure which is computed from Eq. (2).

THE VALUES OF PHYSICAL AND THERMODYNAMICAL VARIABLES OF THE AMBIENT MEDIUM

AM	C_s	Γ	V	ρ	p
Or1	0.01	4/3	0.0	10^3	7.502×10^8
Or2	0.01	5/3	0.0	10^3	6.0009×10^8
Or3	0.01	1.2	0.0	10^3	8.3375×10^8
Or4	0.01	4/3	0.0	10^4	7.5022×10^9
Or5	0.01	5/3	0.0	10^4	6.0009×10^9
Or6	0.01	2	0.0	10^4	5.00049×10^9
Or7	0.1	4/3	0.0	10^4	5.0505×10^9

During the evolution the matter is injected with mildly and highly relativistic velocities along the jet axis continuously. The initial values of density and pressure for injected and surrounding matters are adjusted to get the sound speed equal to required values given in Tables 1 and 2. In practice, we have chosen the constant density and computed the pressure from the following equation for given sound speed C_s ,

$$p = C_s^2 \rho (\Gamma - 1) / \Gamma (\Gamma - 1) - C_s^2 \Gamma, \quad (2)$$

where Γ is the adiabatic index.

2.3. Numerical setups and boundary conditions. The computational grid box expands from $3M$ to $200M$ along the jet axis and from $-40M$ to $40M$ along the perpendicular axis to jet axis. The locations of outer boundaries are far enough from the location of interest to avoid the superior oscillation during the evaluation. The uniformly spaced zones are located along the z and R directions. In our all models, we have chosen $N_z = 3072$ and $N_R = 512$. But it is also confirmed that the dynamical behavior of the jet is not sensitive to the resolutions. On the other hand, the boundaries also play an important role to reach some acceptable physical results at the end of each numerical simulation. We use outflow boundary conditions at all boundaries of computational domain by using zeroth-order extrapolation of all variables.

3. Numerical results. The dynamics of jets from different astrophysical phenomena during the afterglow phase have an important indicator to explain the observational data and to understand the key physical parameters. Relativistic jets may give different morphologies depending on the relevance of the relativistic effects. The over-dense and underdense properties of jets relative to surrounding medium show more internal structures about relativistic jets such as formed

cocoons, head of jets, and shock waves. In this work we concentrate on the dynamical properties and morphology of the relativistic jets for wide range of initial jet parameters.

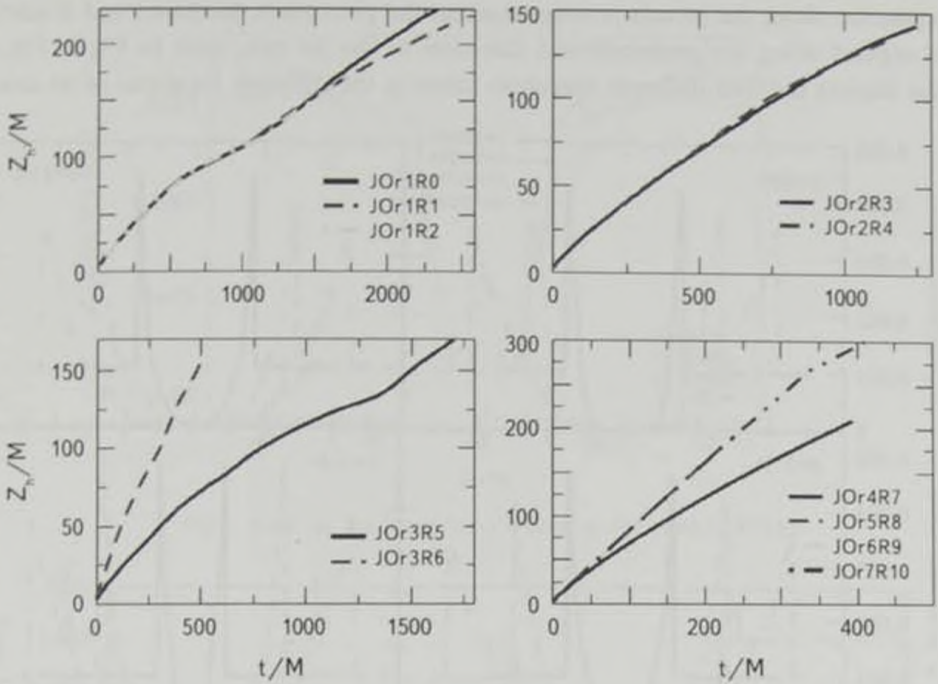


Fig.1. The locations of heads of jets as a function of time for different models in quiescent state

The jets with high Mach number (supersonic jets) propagate inside the stationary ambient matter and they develop double shock shape. While the jet beam moving along the outward direction would be decelerated, the ambient matter which interacts with jet beam would be accelerated. Fig.1 shows the locations of jet's heads as a function of time for different models. As it is expected, the jets propagate in the surrounding medium very fast in case of larger Mach number and the location of head depends on the density ratio between jet and ambient medium, the velocity of jet and Mach number. The jet with higher Mach number or overpressure collimates the jet and minimizes its opening angle. The collimation of matter can cause the formation of skewed shock and it generates pressure which would balance the cocoon's pressure.

Injected jet matter propagates through surrounding medium. The difference between the velocity of the injected matter and back-flow generated as a consequence of jet's head and surrounding broadens the low density region in the medium. In the early time of simulation, jet propagates and expands in this region and generates a thick shear layer which has positive velocities. On the other hand,

the back-flow material interacts with surrounding material and produces the instability and vortices. During these process, working surface creates a bow shock which expands in the external medium. It confines the ram-pressure. The expansion along the jet axis is stopped when the pressure is decreased and it starts to expand along the perpendicular direction to the jet axis, seen in Fig.2. Fig.2 also depicts the four different snapshots taken at the different locations of jet axis,

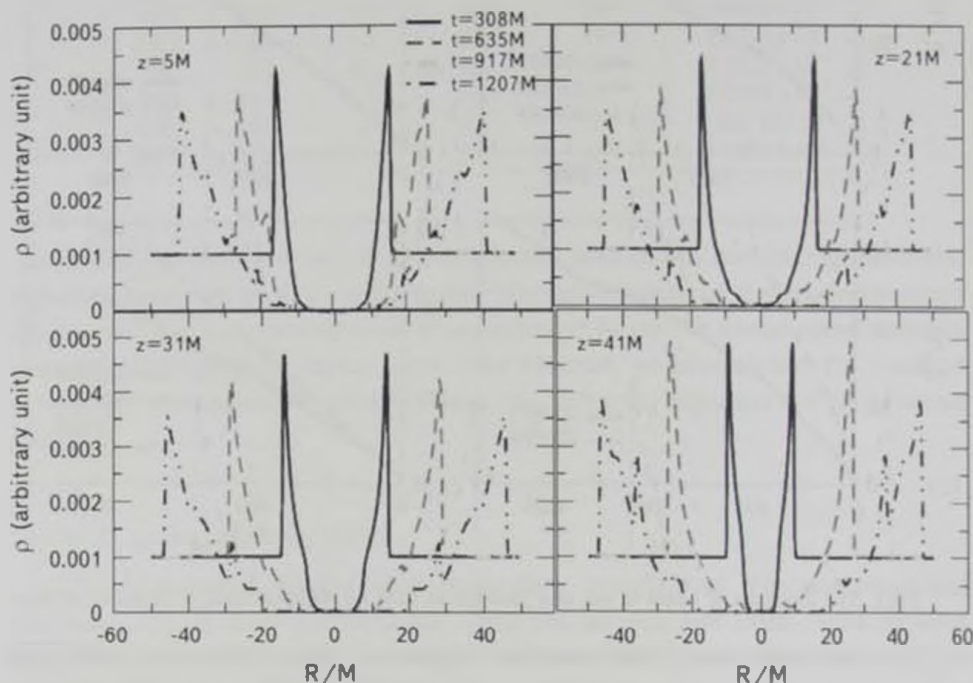


Fig.2. One - dimensional cuts along the R-direction of the rest-mass density at different times for four different values of z in quiescent model $J0r1R0$

$z=5M$, $z=21M$, $z=31M$ and $z=41M$ during the evolution. As it can be seen, the extension along the perpendicular to jet axis is clearly observed for model $J0r1R0$ with adiabatic index $\Gamma=4/3$. But, in case of high adiabatic index $\Gamma=5/3$ for model $J0r2R3$, the extension of dynamic and cocoon overall are almost negligible, seen in Fig.3. Hence, the different adiabatic indices generate noticeable difference in the dynamics of astrophysical jets.

Focusing on the axial structure of jet dynamic, it allows us to compare the densities and Lorentz factors of jets along the propagation axis for different models given in Fig.4. The propagating jet interacts laterally and vertically with external medium due to the density contrast. As a consequence of this interaction, thin shear layer is created. It compresses the head of jet and external shell and produces

a reverse shock, called Mach disk. The Mach disk can cause the increasing in density and decreasing in the Lorentz factor to $W-1$ seen in upper and lower parts of the Fig.4, respectively. During the propagation of jet, the cocoon is formed and it also

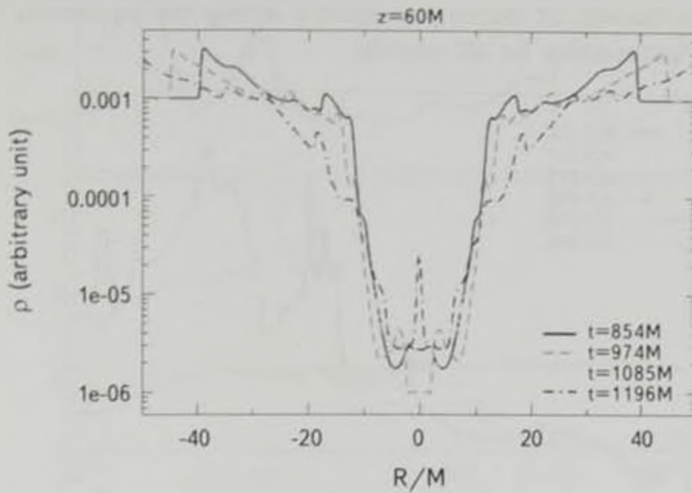


Fig.3. Same as Fig.2 but for $z = 60M$ in the model *JOr2R3*.

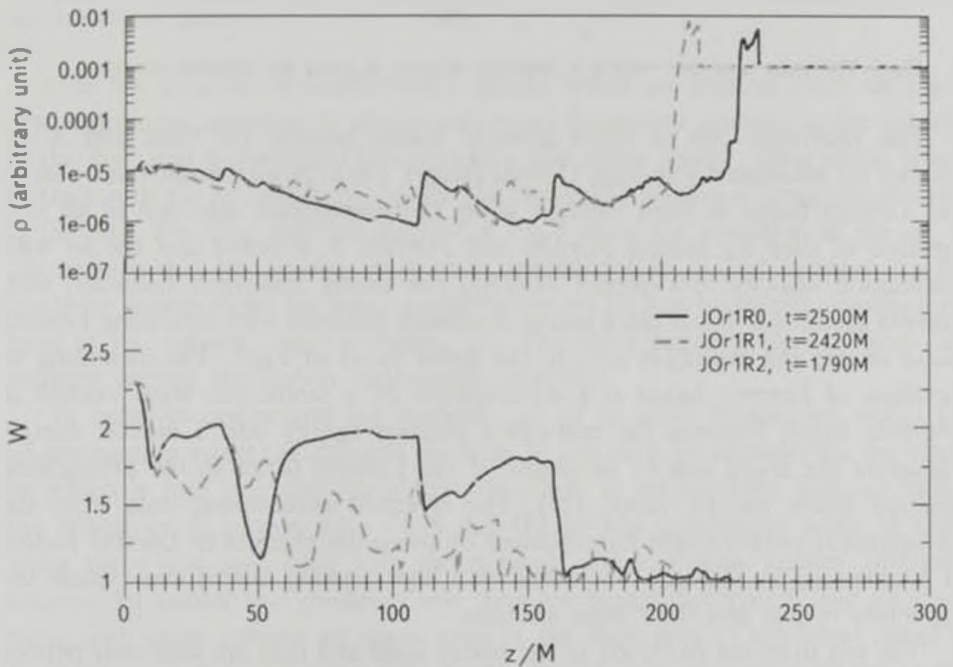


Fig.4. The upper and lower panels display the rest mass density and Lorentz factor of jet along the z axis for the quiescent models *JOr1R0*, *JOr1R1* and *JOr1R2*. The oscillations in ρ and W are clearly observed.

interacts with the propagating jet beam. Hence, due to the expansion and contraction processes inside the jet's structure, the jet undergoes an oscillation in Lorentz factor. Furthermore, the mass accretion rate given in Fig.5 shows that a relatively larger amount of matter is accreted during the interaction of jet's matter with the surrounding for all models.

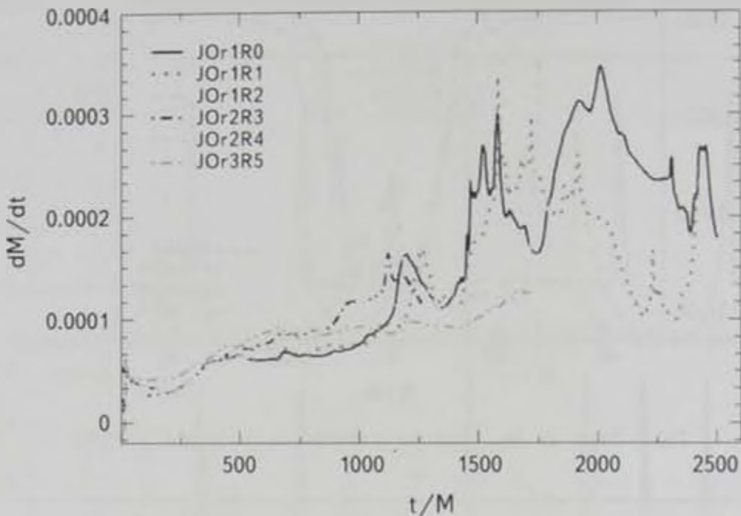


Fig.5. The mass accretion rate as a function of time is given for different models

The relativistic jets in active galactic nuclei, gamma ray burst and X-ray binaries are associated with high Lorentz factors. Fig.6 shows the rest-mass density and Lorentz factor at fixed location along the propagation direction of jet as a function of time for models *JOr3R5* and *JOr3R6*. It is noted that the jet with collimation velocity, 0.9 (model *JOr3R5*) has mildly relativistic behavior, with Lorentz factor ≤ 2 but it has a strong relativistic behavior with increasing Lorentz factor during the evolution seen in the lower panel of Fig.6. The increasing or variation of Lorentz factor is a consequence of a rarefaction wave excited at interface which converts the relativistic thermal energy into a kinetic energy. Therefore the shock can be developed if the Lorentz factor in the propagating material inside the jet varied [22]. The observed acceleration data from the astrophysical system might be explained by using the changes in Lorentz factors of propagating jet features. The beam with high Lorentz factors can explain the variability of jets and their huge energies.

The jets from the AGN are in the parsec scale and they are seen over periods of months to years [1]. We model this type of jet and draw the dynamics of jet for different snapshots shown on Fig.7. As it is seen in this figure that initially underdense and overpressured jets promote through surrounding medium and

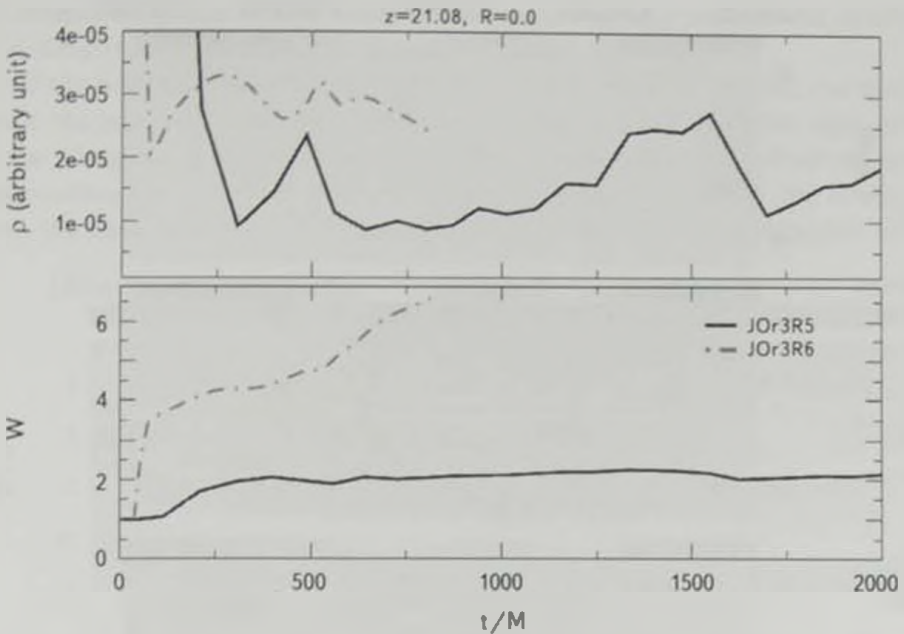


Fig.6. The rest-mass density and Lorentz factor vs. time from the two different models JOr3R5 and JOr3R6 are plotted

develop the numbers of recollimation shocks which are seen as knots on Fig.7. The continuous injection of matter can cause temporary increase in the velocity of the fluid and it develops the rarefaction and shock waves. These waves would interact with the recollimation shocks and create the nonlinear complex structure of the jets. The four different epochs of Fig.7 show the evolution of the jet. It can be seen that perturbation propagate through the jet in first snapshot. In the last three snapshots we see some reestablishments such as backward propagations, head of jet, cocoon, some vortexes, etc. The shear between the jet beam and medium derives the Kelvin Helmholtz instability.

In order to understand the dynamics of jet in more details, we model the jet propagation across the different medium. In this case, we consider the overdense jet which is sent into the surrounding medium in regular time intervals called the pulsed jet. It is seen from Fig.8 that the jet has consecutive series of knots along the z axis associated with the pressure and rest-mass density difference between jet matter and medium, and they are highly collimated. The jet knots move with some average jet speed seen in the right part of the lower panel of Fig.8. The rest-mass densities of the knots are almost standing features during the evolution after they reach the steady state.

Looking at the dynamical behavior of the pulsed type of jets given in Models

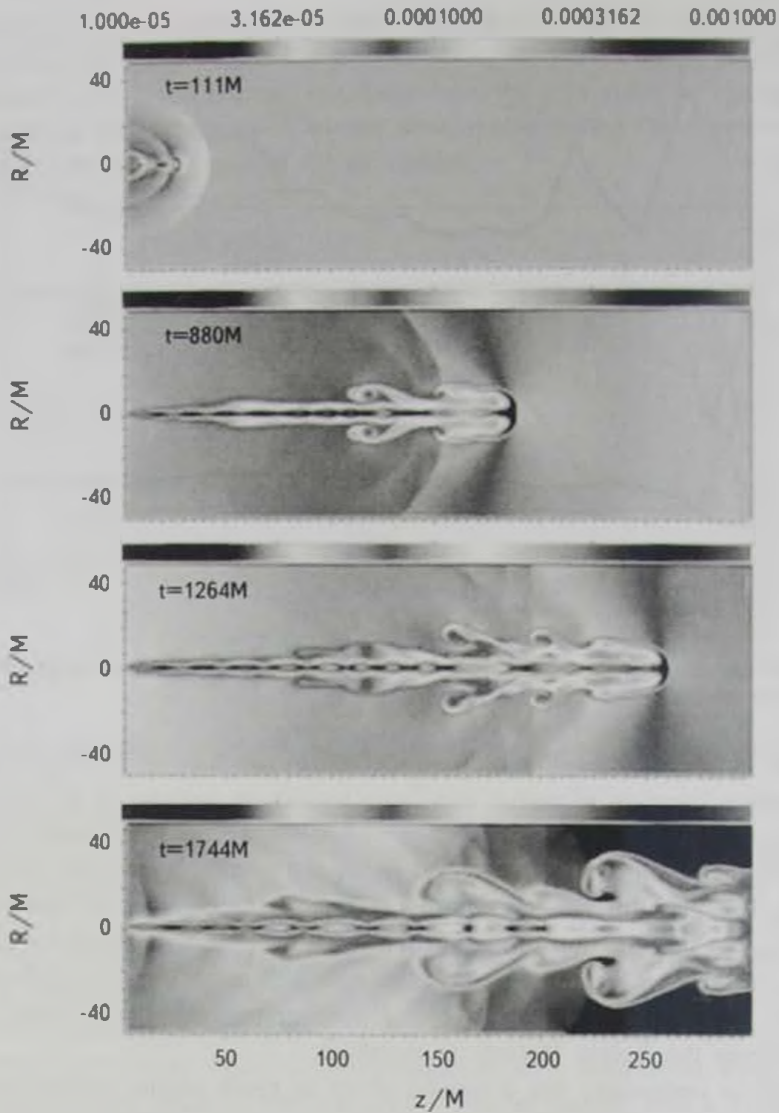


Fig.7 The dynamical change of the logarithmic rest-mass density of the relativistic jets for model *JOr7R13*. The jet propagate through the medium. It is initially overpressured and underdense with respect to the ambient medium.

JOr7R12, *JOr7R13* and *JOr7R14*, we have focused on the 1D cut along the propagation direction of jet. We have observed a regular pattern of knots associated with low Lorentz factor seen in upper part of Fig.9. The intensity of knots created inside the jet dynamics decreases slowly. The number of knots for higher initial collimation velocity of jet is less than the velocity with smaller values. Namely,

the models which has smaller collimation velocity display a more knotty structure than those which has higher collimation velocity.

If the adiabatic index drops below the critical value for the jet, the matter inside the jets spreads sideways [23] and it caused a breaking in the light curve of the afterglow. It was confirmed that the sideways expansion of astrophysical jets pending the afterglow emission changes logarithmically during the evolution [24]. We have seen the same time of spreading with the lower adiabatic index

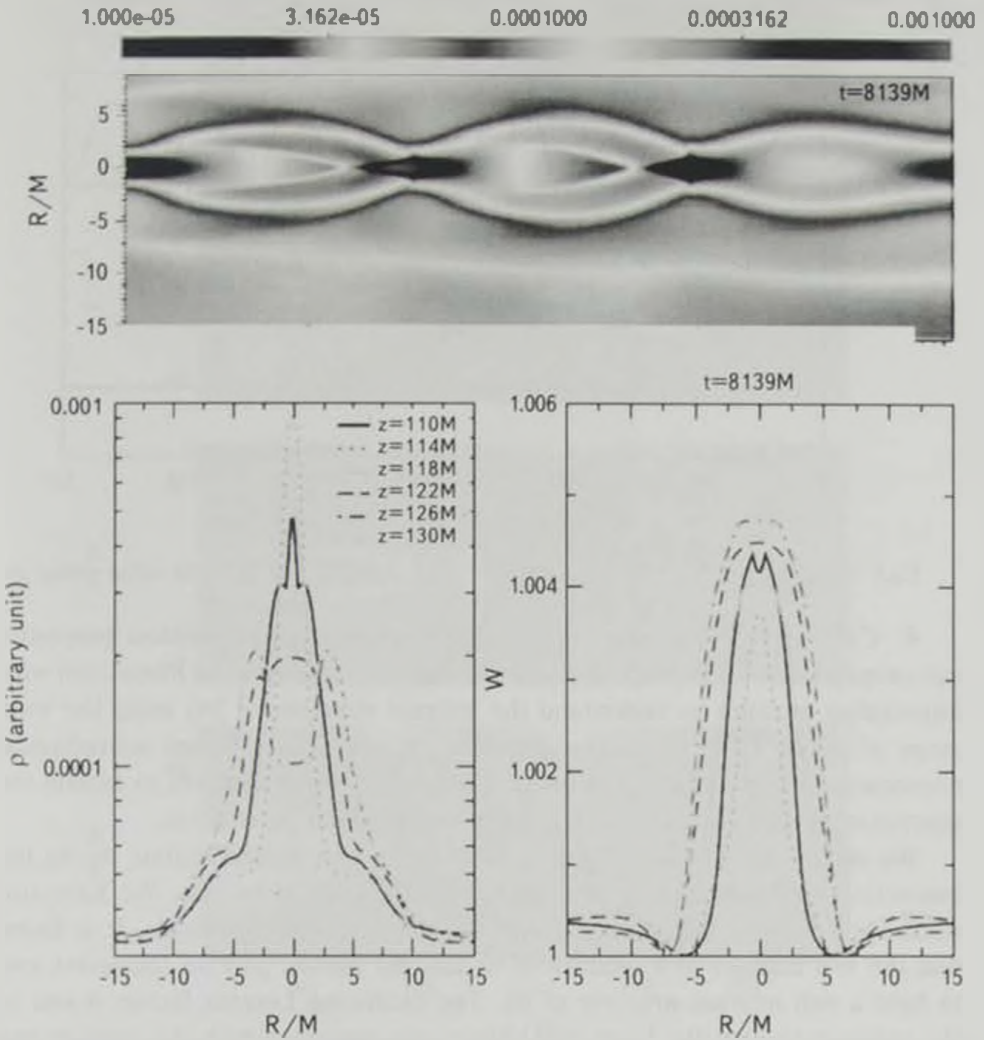


Fig.8. A zoom on small portion of jet knots and 1D cut along the R direction are given for model *JOrR12*. Upper panel: A small portion of the density distribution of 2D jet. Lower panel: the rest-mass density and Lorentz factor are plotted at fixed time, $t = 8139M$ along R for different values of z which are chosen from the upper panel.

in our models when we use the same initial jet opening angles, seen in Fig. 10. Therefore, the rich dynamical structure with vortices, cocoon and backward shocks occurs during the evolution. The higher adiabatic index produces a traveling perturbation which is also adjusted by the temporary increase of the Lorentz factor. The Kelvin-Helmholtz instability might be suppressed by higher Lorentz factor.

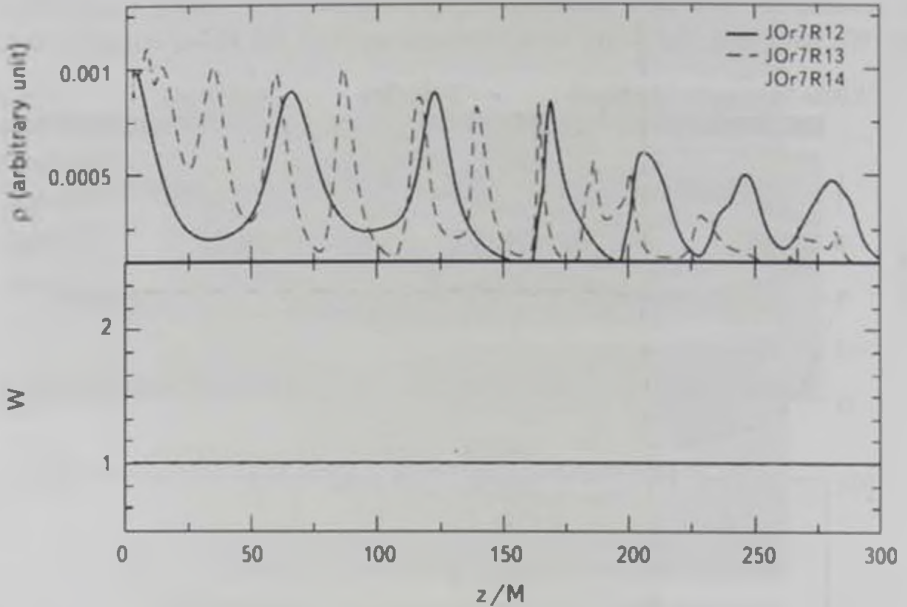


Fig. 9. Same as Fig. 4 but it is for models *JO7R12*, *JO7R13* and *JO7R14* called pulsed jet.

4. Conclusion. We have presented the morphology, dynamical properties and propagation of relativistic jets in 2-dimensional space and its interaction with surrounding medium to understand the internal structure of jets using the wide range of initial parameters. The dynamics of jets from different astrophysical phenomena during the afterglow phase have an important indicator to explain the observational data and to understand the key physical parameters.

We observe the number of jets features over a long period of time during the interaction with surrounding medium for different initial models. We have also studied the Lorentz factor destructions for some interesting models. It is found that the real changes and oscillations in Lorentz factors play an important role to have a rich internal structure of jet. The oscillating Lorentz factors is one of the indicators to have the knots along the z axis associated with the pressure and rest-mass density. The knots created inside the jets move with some average jet speed. The rest-mass densities of the knots are almost standing features during the evolution after they reach to the steady state.

The relativistic effect of jets seems to trigger the some of the properties of morphology of the system. If the injected matter of jet has almost similar pressure with their surroundings, the jets have little internal structure. Hence more smooth

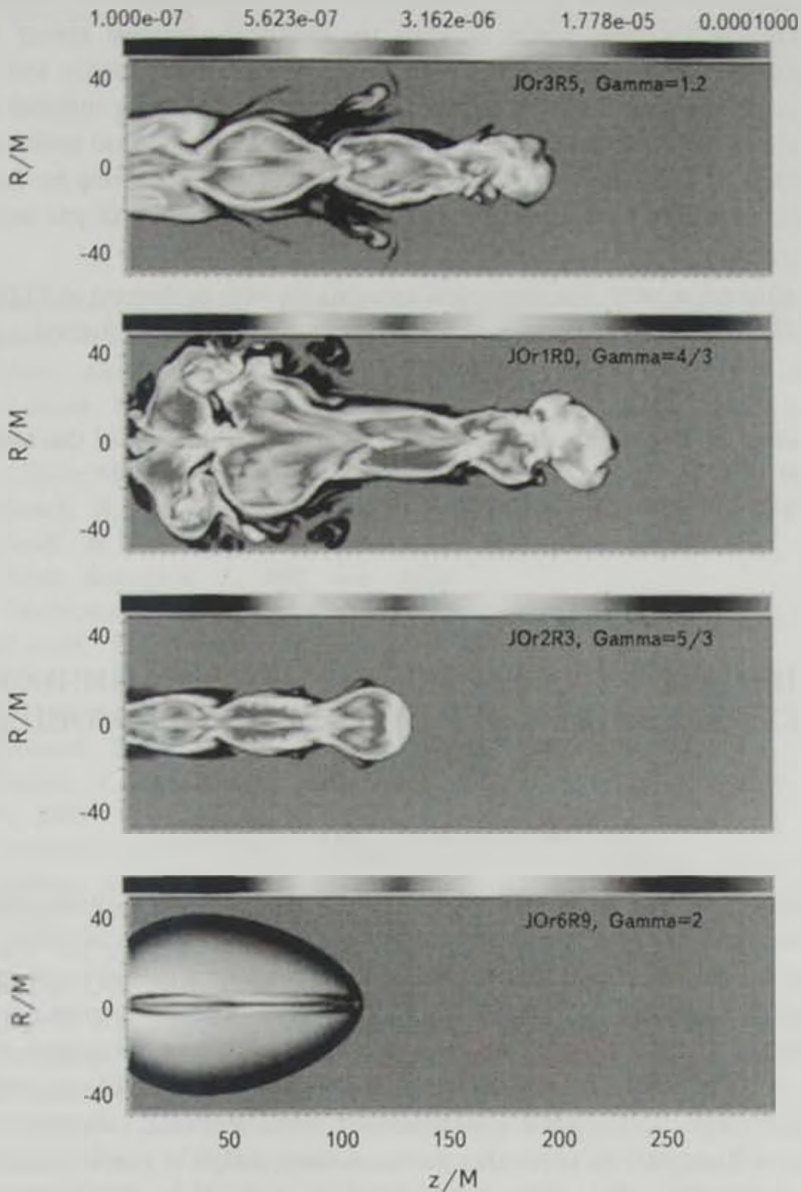


Fig.10 The logarithmic densities of relativistic jets for different adiabatic indices and atmospheres for given models, JO_r3R5 , JO_r1R0 , JO_r2R3 and JO_r6R9 . The jets are initially overpressured with respect to the ambient medium and dynamics of jets are plotted for densities which are represented with color on top of the $R-z$ plane.

cocoons are formed near the jet's head. Overpressured models with highly relativistic effects (high Lorentz factor for beam) display more complex dynamics of jet with extended cocoons and it causes increasing the Lorentz factors with time. The increasing or variation in the Lorentz factor is a consequence of a rarefaction wave excited at interface which converts the relativistic thermal energy into a kinetic energy. Therefore the rearfaction wave, contact discontinuity and shock waves can be developed if the Lorentz factor in the propagating material inside the jet varies. The observed acceleration data from the astrophysical system might be explained by using the change in Lorentz factors of propagating jet features. The beam with high Lorentz factors can explain the variability of jets and their huge energies.

Acknowledgments. The numerical calculations were performed at TUBITAK ULAKBIM High-Performance and Grid-Computing Center (TR-Grid e-Infra-structure).

¹ College of Engineering and Technology, American University of the Middle East (AUM), Egaila, Kuwait, e-mail: orhan.donmez@aum.edu.kw

² Nigde University, Nigde Turkey, 51200

ЧИСЛЕННОЕ МОДЕЛИРОВАНИЕ АСТРОФИЗИЧЕСКИХ ДЖЕТОВ. ВЗАИМОДЕЙСТВИЕ С ОКРУЖАЮЩЕЙ СРЕДОЙ

О.ДОНМЕЗ¹, А.АКТАС², У.ИЛТЕР²

Распространяясь, астрофизические джеты в результате взаимодействия с веществом окружающей среды переносят большое количество энергии. Такое взаимодействие оказывает решающее влияние на их динамику и эволюцию. Оно может привести к образованию вертушки джета, энергия которой диссипирует. В работе численно моделируется эволюция динамики джета с целью выявить влияние критических параметров (числа Маха, скорость джета, плотность, давления ускоряющегося джета и среды, скорость звука и множитель Лоренца) на вертушку джета, кокон, вихри и удары. Когда джет распространяется в более плотной среде, мы видим, как он замедляется и приобретает более сложную форму. В разреженной среде обратные потоки и коконы практически не образуются. Мы моделировали также пульсообразные джеты, распространяющиеся в более плотной среде, и обнаружили у них

сложную внутреннюю структуру, состоящую из коконов, узлов, вихрей и т.д. Они могут объяснить структуру джетов, видимых в дугах Херbiga-Apo, и прото-джетов у XZ Tau.

Ключевые слова: численная теория относительности: астрофизические джеты: окружающая среда: структура джетов

REFERENCES

1. *M. Boettcher, D.E. Harris, H. Krawczynki*, *Relativistic Jets from Active Galactic Nuclei*, Wiley, 2012.
2. *M. Ribo*, ASPC, **340**, 421, (astro-ph/0402134), 2005.
3. *R.P. Fender, T.M. Belloni, E. Gallo*, *Mon. Not. Roy. Astron. Soc.*, **355**, 1105, 2004.
4. *Y. Uchida, K. Shibata*, PASJ, **37**, 515, 1985.
5. *K.A. Miller, J.M. Stone*, *Astrophys. J.*, **489**, 890, 1997.
6. *T. Kudoh, R. Matsumoto, K. Shibata*, *Astrophys. J.*, **508**, 186, 1998.
7. *C. Fendt, M. Cemeljic*, *Astron. Astrophys.*, **395**, 1045, 2002.
8. *C. Fendt*, *Astrophys. J.*, **692**, 346, 2009.
9. *A. Tchekhovskoy, J.C. McKinney*, *Mon. Not. Roy. Astron. Soc.*, **423**, L55, 2012.
10. *J.M. Stone, M.L. Norman*, *Astrophys. J.*, **413**, 210, 1993.
11. *A. Rosen, M.D. Smith*, *Mon. Not. Roy. Astron. Soc.*, **343**, 181, 2003.
12. *P.E. Velazquez, A.C. Raga*, *Astron. Astrophys.*, **362**, 780, 2000.
13. *O. Dönmez, R. Kayali*, *Appl. Math. Comput.*, **182**, 1286, 2006.
14. *P. Bordas, V. Bosch-Romon, J.M. Paredes, M. Perucho*, *Astron. Astrophys.*, **497**, 325, 2009.
15. *M. Perucho, V. Bosch-Romon, D. Khangulyan*, *Astron. Astrophys.*, **512**, L4, 2010.
16. *P. Mimica, M.A. Aloy, J.M. Rueda-Becerril et al.*, *IOP Conference Series*, **454**, 012001, 2013.
17. *Y. Ha, C.L. Gardner, A. Gelb et al.*, *J. Sci. Comput.*, **24**, 29, 2005.
18. *Y. Ha, C.L. Gardner*, *J. Sci. Comput.*, **34**, 247, 2008.
19. *J.E. Krist, K.R. Stapelfeldt, J.J. Hester et al.*, *Astrophys. J.*, **136**, 1980, 2008.
20. *C.L. Gardner, S.J. Dwyer*, *Acta Mathematica Scientia*, **29B(6)**, 1677, 2009.
21. *O. Dönmez*, *Astrophys. Space Sci.*, **293**, 323, 2004.
22. *F. De Colle, J. Guillochon, J. Naiman et al.*, *Astrophys. J.*, **760**, 103, 2012.
23. *R. Sari, T. Piran, J.P. Halperen*, *Astrophys. J.*, **519**, L17-L20, 1999.
24. *H. van Eerten, A. MacFadyen*, *Astrophys. J.*, **751**, 155, 2012.